Damage Detection and Localization in Structures: A Statistics Based Algorithm Using a Densely Clustered Sensor Network

Elizabeth L. Labuz[1], Shamim N. Pakzad[2], and Liang Cheng[3]

[1]Graduate Student, Department of Civil and Environmental Engineering, Lehigh University, 117 ATLSS Drive, Bethlehem, PA 18015; PH (610) 758-4543; FAX (610) 758-5553; email: elabuz@lehigh.edu
[2]P.C. Rossin Assistant Professor, Department of Civil and Environmental Engineering, Lehigh University, 117 ATLSS Drive, Bethlehem, PA 18015; PH (610) 758-6978; FAX (610) 758-5553; email: pakzad@lehigh.edu
[3]Associate Professor, Department of Computer Science and Engineering, Lehigh University, 326 Packard Lab, Bethlehem, PA 18015; PH (610) 758-5941; email: cheng@cse.lehigh.edu

ABSTRACT

Damage prognosis for structural health monitoring is a challenging and complex research topic in civil engineering. Early and accurate damage detection is essential to maximizing the useful life of structures. The use of densely clustered sensor networks provides promising applications in the analysis of structural components and identification of local damage. The proposed localized damage detection method utilizes a linear regression analysis to monitor changes in the linear behavior of a structure with the onset of damage. The structural responses at various sensor locations along a structure are compared to those of other locations and pair-wise influence coefficients are estimated. These coefficients serve as damage indicators when damaged values are compared to healthy-state values. By statistically comparing the change in influence coefficients, structural damage can be accurately and effectively identified. The method is verified using simulations and an experimental prototype of a local beam-column connection, as well as a simulated model of a two-span bridge girder.

INTRODUCTION

Structural health monitoring (SHM) plays an integral role in maintaining the integrity of important civil, mechanical, and aerospace engineering systems. Structures experience a number of dynamic influences on a daily basis ranging from typical ambient vibrations to more extreme wind and earthquake loadings. Whether the damaging effects of these load cases are visible immediately or appear more gradually in time, it is important to be able to detect the damage before it becomes detrimental to the entire structure and its surroundings. Not only will money be saved by being able to repair more manageable damages at earlier detection, but also fatal catastrophes can be prevented. As an increasing number of structures are beginning to reach the limit of their service lives, the need for effective, efficient, and affordable damage detection methods is becoming more apparent.

Traditional non-destructive evaluation (NDE) techniques include but are not limited to visual inspection, liquid penetrant, magnetic particle, radiography, eddy

currents, ultrasonic waves, acoustic emission, and infrared thermography (Trimm 2007). While these methods are useful in certain circumstances, they require *a priori* knowledge of the location of damage and are subject to the trained eye of the inspector. Also, in order to implement these techniques one must have direct access to the location of damage, which may be difficult to reach. Furthermore, NDE techniques are costly, difficult to use with complex equipment, and provide only a temporary means of SHM.

Both advancements in sensor technologies as well as improved understanding of the modal properties of structures have given rise to vibration-based damage identification methods. These methods find a basis in the vibration behavior of a structure, namely the connection between the modal parameters of a structural system—natural frequencies, mode shapes, and modal damping—and its physical properties—mass, stiffness, and damping (Doebling *et al* 1998; Alvandi and Cremona 2006). Parametric changes signify changes in the physical properties, i.e. structural damage in the form of mass or stiffness loss. Also, the advancements of wireless networks make it possible to implement these vibration-based methods on a semi-permanent basis for continuous monitoring of structures.

However, current SHM practices involving global-based damage detection require knowledge of specific structural properties, including mass, stiffness, or damping ratio, for which it is often difficult to determine correct values (Koh *et al* 1995; Morassi and Rovere 1997; Sohn and Law 1997; and Ratcliffe 1997). Additionally, global detection techniques, which are based on global properties, are not sensitive to local damage and, therefore, cannot determine damage locations. Other proposed local damage detection methods, for example the damage locating vector (DLV) method (Bernal 2002), also require the knowledge of structural properties or require homogeneity of the structural properties as in the two-dimensional gapped smoothing method (Yoon *et al* 2005).

An effective damage detection method has been proposed that is sensitive to local damage (Labuz *et al* 2010). The method uses vibration responses collected via densely clustered sensors to achieve localized damage detection without the need for exact knowledge of structural properties. Influence coefficients, obtained from linear regression between pairs of node responses, are used as the index for determining the existence of damage. This study presents both simulated and experimental results to demonstrate the effectiveness of the proposed local damage detection method.

DAMAGE DETECTION ALGORITHM

The algorithm implemented is based on the assumption that a structure exhibits linear behavior, and is thus applicable for identifying damage in structures that fall within this category. In order to capture this behavior, linear regression analysis is used to find pair-wise influence coefficients, α_{ij}, between two nodes i and j, based on the structural response data u_i and u_j at time instance t_k with ε_{ij} and β_{ij} being time-variant and invariant linear regression parameters along with α_{ij} to be estimated as follows:

$$u_j(t_k) = \beta_{ij} + \alpha_{ij} \cdot u_i(t_k) + \varepsilon_{ij}(t_k).$$

The structural response will change as damage occurs, which is then reflected in the influence coefficients. Therefore, the comparison of the resulting influence coefficients from the initial undamaged state with those of the damaged state of the structure serves as a *damage indicator* when it yields a significant change in the value of the coefficients from state to state. This characteristic allows for the identification of the damage location by observing the pattern of influence coefficients exhibiting significant changes. Because this method only involves processing of the structural response, this is an output-only method and, thus, can be easily applied regardless of loading conditions. Figure 1 outlines the procedure for the damage detection algorithm.

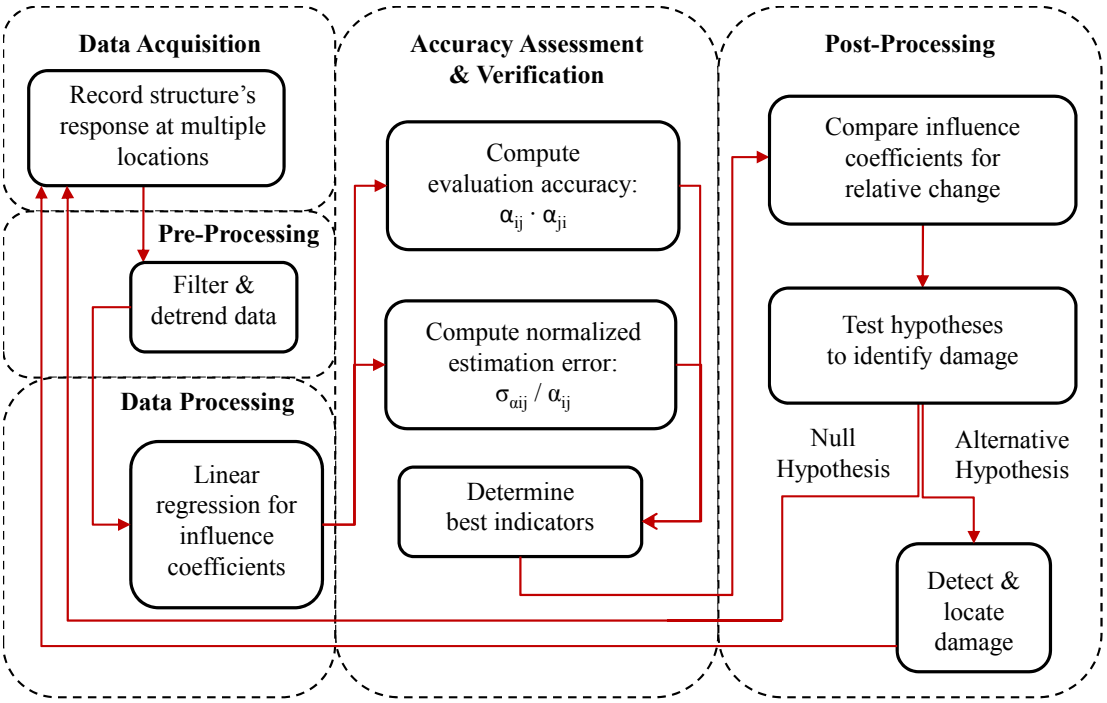

Figure 1. Damage detection algorithm procedure.

INFLUENCE COEFFICIENTS AND NORMALIZED ESTIMATION ERROR

Once the coefficients have been calculated, the accuracy of the data must be assessed and verified before damage detection can be performed. By minimizing the error in the parameters, the occurrence of false alarms will also be minimized. Two parameters are considered for this purpose: the evaluation accuracy and the normalized estimation error associated with each pair-wise coefficient. The product of influence coefficients α_{ij} and α_{ji}, yields the evaluation accuracy, EA_{ij}, of these coefficients, indicating which node responses are linearly related to one another with the least amount of regression error, ε_{ij}, and thus are more accurate predictors. An evaluation accuracy of 1.0 signifies a strong accuracy of estimation, while a product of less than 1.0 corresponds to progressively higher values of noise and nonlinear behavior of the physical structure.

The second parameter that is used for data verification is normalized estimation error, which is calculated by

$$\gamma_{ij} = \frac{\sigma_{\alpha_{ij}}}{\alpha_{ij}}.$$

Normalized estimation error allows for a direct comparison of the amount of error exhibited within the measured data. A low estimation error will correspond to a more accurate predictor. Based on these two parameters the strongest damage indicating influence coefficients are identified for use in damage detection. These coefficients are post-processed and monitored for significant changes to localize the damage.

SIMULATED BEAM-COLUMN CONNECTION

A simulated model is used to demonstrate the application of this method. Consider a simple beam-column connection, representing a local joint, with nine node locations, as shown in Figure 2. The column portion of the joint is fixed at both ends while the beam cantilevers out from the centerline of the column. Two simulation conditions were performed which include (1) an undamaged baseline condition and (2) a damaged condition, characterized by a 40% reduction in the beam stiffness. For each of these models, displacement data was simulated for a white noise excitation applied at the free end of the beam in the y-direction. Measurement noise was accounted for by adding additional noise to the response.

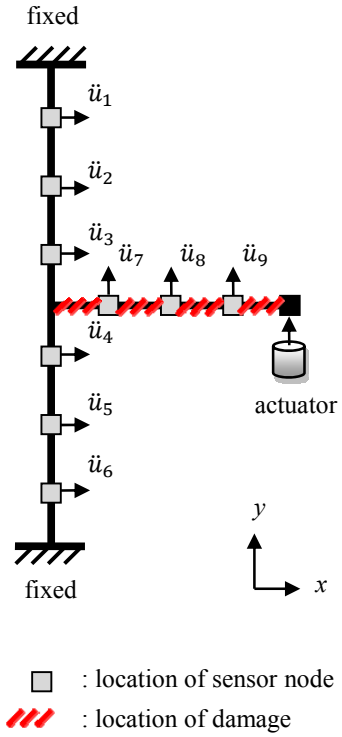

Figure 2. Local beam-column joint with nine node locations used for simulated beam-column model.

SIMULATION RESULTS

The algorithm was then applied to the simulated displacement data and the parameters were extracted. A selection of the influence coefficient changes are shown in Figure 3. The influence coefficients $\alpha_{ij},\ 1 \leq i,j \leq 6$ all experience very small (less than 1%) changes between the undamaged and damaged states. This implies that the physical relationship between these nodes has not changed. However, the coefficients of nodes 1 through 6 paired with nodes 7, 8, and 9 show relative changes between 30-40%. When nodes are on opposite sides of the damage, i.e. nodes 1 through 6 are on the undamaged column, while nodes 7, 8 and 9 are on the damaged beam, the physical relationship between the paired nodes change. The beam experiences more flexibility in the form of higher displacements, whereas the column nodes see small displacements similar to the undamaged state. This physical change is reflected in a more significant relative change in the value of influence coefficients. Furthermore, the influence coefficients $\alpha_{ij}, 7 \leq i,j \leq 9$ also experience changes in coefficients between 3-10%. This signifies that the physical properties of the structure between α_{78}, α_{79}, and α_{89} have changed. Therefore, damage must exist between these nodes. This is consistent with the known damage condition. Thus, the application of influence coefficients and local damage indicators is demonstrated.

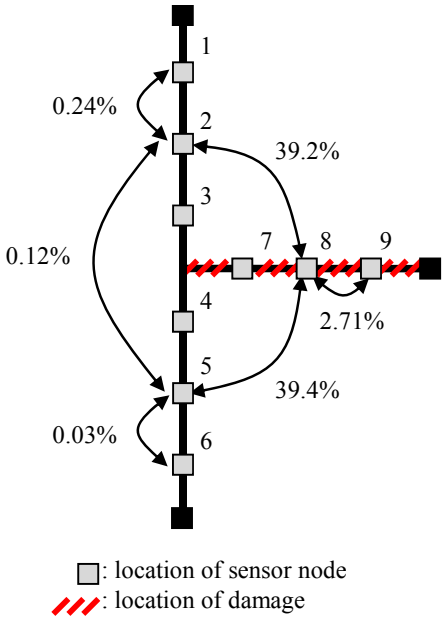

Figure 3. Relative change in pair-wise influence coefficients for the simulated beam-column structure.

EXPERIMENTAL BEAM-COLUMN CONNECTION

A small-scale steel beam-column connection, based on the simulated model, was constructed in the ATLSS Center at Lehigh University and was used for experimental verification of the algorithm. As is shown in Figure 4, the two ends of the column have fixed supports and the beam cantilevers from the centerline of the column. The intention was to model the beam-column connection area in which this prototype

represents only a portion of these members. The free end of the cantilever was attached to an actuator and excited by harmonic force at a 15 Hz forcing frequency, and the acceleration responses were collected at each of the nine sensor nodes. Furthermore, to avoid nonlinear behavior of the elements, an amplifier controlled the amplitude of the excitations. This portion of the experiment served to establish a baseline response for the undamaged structure.

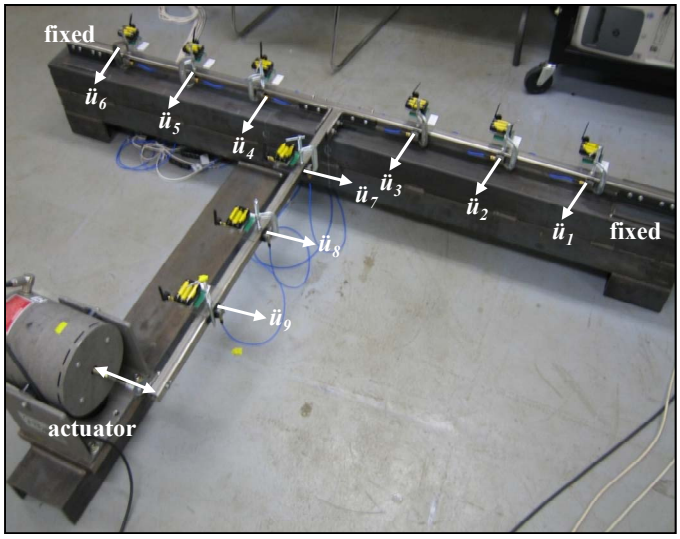

Figure 4. Experimental beam-column instrumented with nine tethered accelerometers.

For the second portion of the experiment, the beam member was replaced by a member of 40% reduced wall thickness in order to simulate damage to the structure. The excitations were repeated similarly to the undamaged case.

Acceleration data at each sensor location was collected at a 200 Hz sampling rate and 0.005 sec time step, with each test lasting 10 seconds total. Both the undamaged and damaged structures were tested 50 times, for a total of 100 tests, each containing 2000 samples per sensor location. All data was pre-processed and influence coefficients were computed to locate the damage.

EXPERIMENTAL BEAM-COLUMN RESULTS

Once the 72 influence coefficients were calculated from the acceleration data, they were assessed to identify the most significant indicators to be used for damage detection. This involves two parameters: evaluation accuracy, *EA*, and normalized estimation error, γ. By inspection of these parameters, eight different trends can be identified in the undamaged and damaged parameters, with lower estimation errors coinciding with greater evaluation accuracies and vice versa. These trends have been designated as eight different regions, whose mean values are presented in Table 1. Region 1 in the table corresponds to the least estimation error and highest accuracy, and region 8 corresponds to the greatest estimation error and lowest accuracy. Parameters in region 1, consisting of $\alpha_{ij},\ 7 \leq i,j \leq 9$, are the most accurate and have the least error. This is a reasonable outcome as nodes 7, 8, and 9 are all located in a

row along the same structural element (the beam). Therefore, the accelerations at node 7, for example, will be more highly correlated to those at node 8 or 9.

Table 1. Average Estimation Error (γ) and Evaluation Accuracy (*EA*).

Region	Influence Coefficients	γ_{ij} Average	EA_{ij} Average
1	α_{78}, α_{79}, and α_{89}	0.0002	0.9999
2	α_{23} and α_{45}	0.0015	0.9947
3	α_{27}, α_{28}, α_{29}, α_{37}, α_{38}, α_{39}, α_{47}, α_{48}, α_{49}, α_{57}, α_{58}, and α_{59}	0.0044	0.9554
4	α_{12}, α_{13}, α_{46}, and α_{56}	0.0057	0.9377
5	α_{17}, α_{18}, α_{19}, α_{67}, α_{68}, and α_{69}	0.0074	0.8997
6	α_{24}, α_{25}, α_{34}, and α_{35}	0.0093	0.8379
7	α_{14}, α_{15}, α_{26}, and α_{36}	0.0114	0.7903
8	α_{16}	0.0161	0.6626

On the contrary, region 8, which consists of parameter α_{16}, exhibits the poorest accuracy and the greatest estimation error. This can be accounted for by the fact that each of these nodes is located at either end of the column near the fixed connections. These boundary conditions create large additional noise, which contributes to the fact that α_{12} or α_{56} exhibit lower accuracy than α_{78} or α_{89} despite the similar configuration of the nodes with respect to one another. Figures 5(i) and (ii) show examples of α, *EA*, and γ results from regions 1 and 8, respectively. Figure 5(i) shows that the *EA* is almost equal to unity and the γ is almost equal to 0 for region 1, while Figure 5(ii) shows a much lower *EA* and a noticeably higher γ for region 8. Moreover, Figure 5(i) shows a more decisive change in the influence coefficient value than Figure 5(ii). Based on similar data for all 8 regions, it can be concluded that regions 1 through 4 contain useful damage indicators. On average, these influence coefficients exhibit accuracy greater than 93% and estimation error less than 0.006.

The experimental results of the relative changes in the influence coefficients, α_{ij}, between the undamaged and damaged tests are shown briefly in Figure 6. Observing these coefficient changes is the first step in post-processing the data. The changes associated with α_{78}, α_{79}, and α_{89}, which are 8%, 12%, and 4% respectively, are potential indicators of a property change between nodes 7 and 9. This is consistent with the damage, or stiffness reduction, that was created along the full length of the beam portion of the test structure.

The coefficients of region 2, α_{23} and α_{45}, experienced 3% and 8% changes. This is less consistent with what would be expected in comparison to the very low (less than 1%) changes that were seen in the simulated results. One major cause of this is ambient noise, which is difficult to control in an experimental setting, but even more so in a real structure.

Influence coefficients from region 3 were more in line with the prediction of the simulated results, with the exception of α_{49} (2%) and α_{57} (3%), which were low compared to the 5-40% range of the others. Again, these two discrepancies are likely accountable to noise. However, the majority of the coefficients in this region showed noticeable fluctuations from the undamaged state to the damaged state. These changes, along with the model results, show that nodes on opposite sides of the damage location experience the largest changes, which is consistent with the simulated results. Again,

the changes in coefficients point to the location of damage in the structure (i.e. damage between nodes 2 and 7, 3 and 8, and so forth).

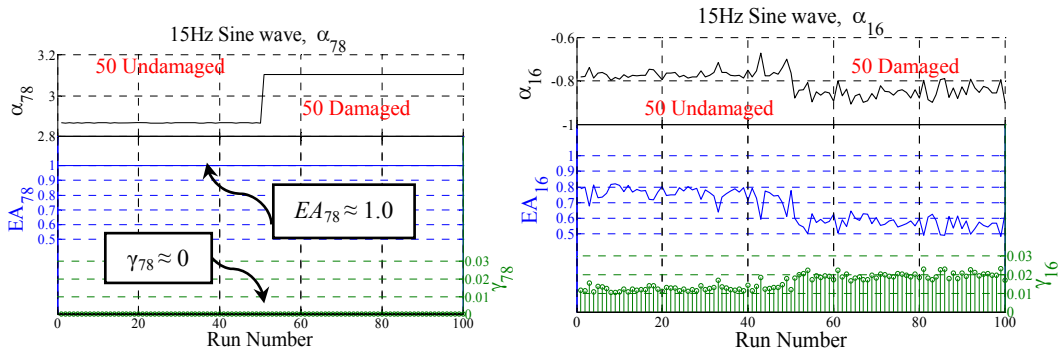

(i) (ii)

Figure 5. Comparison of *α*, *EA*, and *γ* results: (i) Region 1 and (ii) Region 8.

While the results for the first three trend regions were mostly consistent with the simulated results, the remaining regions were not as consistent. A prime example is region 6, consisting of parameters α_{24}, α_{25}, α_{34}, and α_{35}. According to the model, these coefficients, whose nodes are all located on the same side of the damage, should experience very little fluctuation from the undamaged to damaged states. However, their experimental changes range from 12-20%. Recall that in the previous verification stage region 6 showed the third lowest accuracy and the third highest error; therefore, these coefficients are not considered to be significant damage indicators and can be neglected.

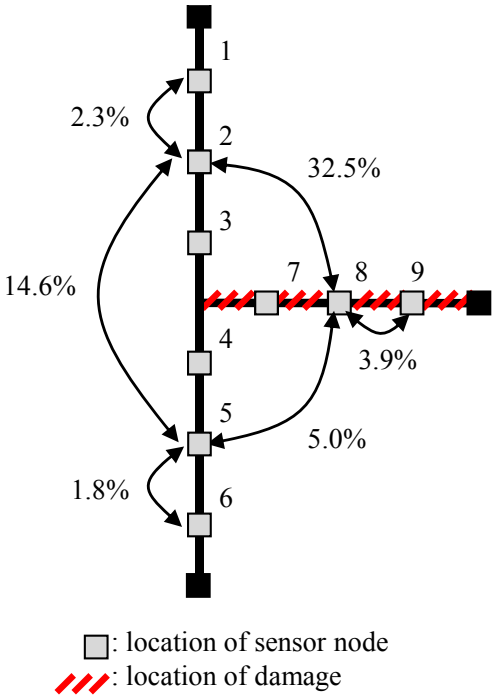

Figure 6. Relative change in pair-wise influence coefficients for the experimental structure.

SIMULATED TWO-SPAN GIRDER

In order for the proposed damage detection method to be adequately verified for practical application, it must be applied to more complex structures. Therefore, a small-scale two-span steel bridge girder has been simulated. The girder was modeled as a two-dimensional frame with short columns with fixed supports and uneven spans as shown in Figure 7. This configuration was chosen as it can model the behavior of a bridge girder, as well as that of a building frame. Furthermore, the uneven spans allow for more variety in the results and damage scenarios. The model has 21 total nodes, which coincide with the sensor locations, with six at each corner joint and nine at the center joint. A white noise excitation was applied in the x-direction to produce displacement responses at each node. Measurement noise was accounted for by adding random noise to the response. Two simulation conditions were considered which include (1) an undamaged baseline condition and (2) a damaged condition, characterized by a 50% reduction in the stiffness of an 8-inch portion of the center column between node C7 and the beam as noted in Figure 7. It is important to note that this corresponds to only a 0.7% decrease in stiffness of the column as a whole. The rest of the structure maintains the same stiffness properties as the undamaged structure.

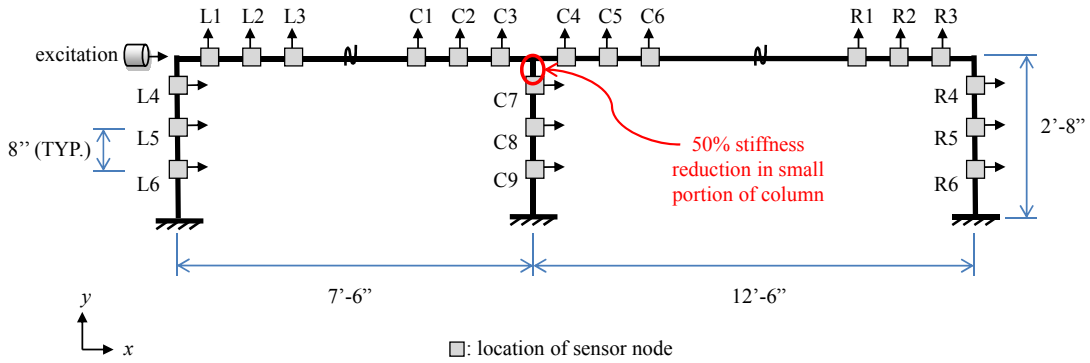

Figure 7. Simulated two-span bridge girder with 21 sensor node locations.

SIMULATION RESULTS

Results were generated considering 100 (50 undamaged, 50 damaged) separate sets of 2000 simulated samples per node. The damage detection algorithm was then applied to the simulated displacement data and the influence coefficients were determined. The plots in Figure 8 demonstrate pair-wise relationships that show (i) the significant change in coefficients on opposite sides of the damage (C2 to C8) versus (ii) the negligible change in coefficients on the same side of the damage (L5 to L6). Even with added noise, both examples show high accuracies and low errors. Thus, both coefficients are considered as significant damage indicators. These change patterns are consistent with those found in the beam-column simulations and experiments.

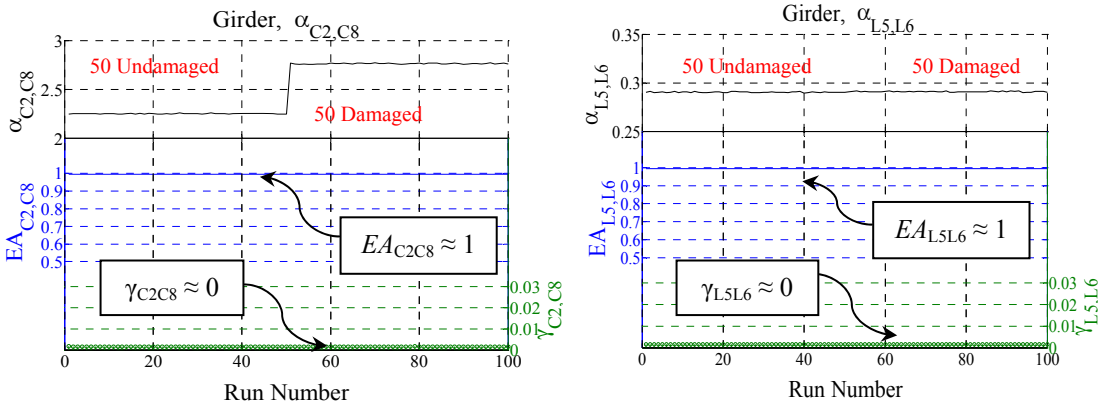

Figure 8. Comparison of *α*, *EA*, and *γ* for (i) nodes surrounding damage and (ii) nodes remote from damage.

Figure 9 shows the average change in influence coefficients throughout the structure resulting from the damage. As can be seen, the center beam nodes (C1 through C6) change more than two or three times that of the other nodes. This is consistent with the known 50% localized stiffness reduction at the central connection. Therefore, the algorithm is sufficient in identifying the general location of damage within the structure as a whole, even though the overall stiffness reduction of the structure was negligible.

Furthermore, the modal properties of the structure change insignificantly with the occurrence of damage at the central joint. This can be seen in Table 2, which shows the modal frequencies of the first three modes for the undamaged and damaged conditions. The percent changes range from approximately 0.5% to 1.5%. These minor changes would be undetectable in any modal-based global detection method with consideration of reasonable errors. However, the proposed localized method detects the damage effectively regardless of minimal changes in global properties.

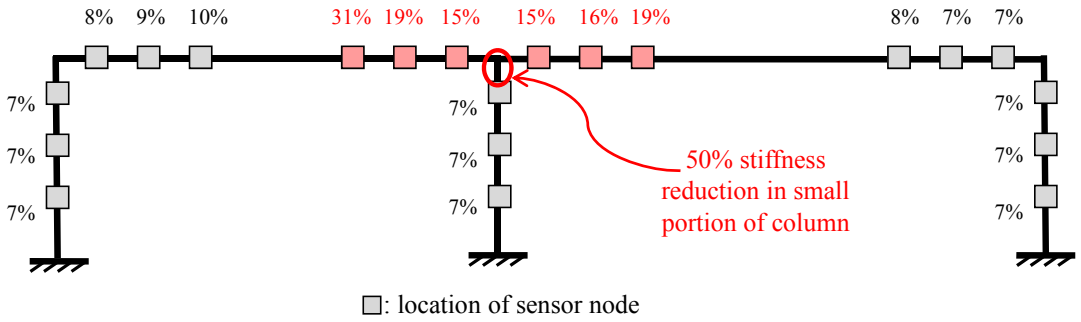

Figure 9. Average relative change in pair-wise influence coefficients for the simulated beam-column structure.

Table 2. Modal frequencies in Hz for the undamaged and damaged models.

	Undamaged	Damaged	% Change
Mode 1	2.67 Hz	2.64 Hz	1.16%
Mode 2	4.45 Hz	4.42 Hz	0.59%
Mode 3	6.81 Hz	6.70 Hz	1.53%

CONCLUSION

A densely clustered sensor network was successfully implemented for local damage detection of both a simulated model and experimental prototype of a steel beam-column connection. The proposed output-only method effectively used linear regression to estimate influence coefficients from vibration-induced acceleration responses of the structure. Changes in the influence coefficients correctly reflected changes in the vibration properties of the structure, thus, revealing the existence and location of damage. Although the experimental structure exhibited more noise error than the simulated results, both the simulation and the experiments identified the location of damage.

Additionally, results showed a significant difference in performance between coefficients with high EA and low error and those with low EA and high error. Therefore, coefficients must be evaluated for strong damage indicating characteristics as this noticeably contributes to the effectiveness of damage detection. In real-world applications earlier damage detection will allow for more manageable repairs and reduce the risk of structural failures.

Finally, a structure in the form of a bridge girder with two unequal spans was simulated. This model was used to investigate the application of the algorithm for more complex structures with more realistic damage scenarios. Using simulated displacement data and applying the algorithm, the resulting influence coefficients correctly identified the central local joint as the location of damage. This is especially significant because both global stiffness and modal frequencies of the structure remained nearly unaffected by the occurrence of damage. This suggests that other detection methods that are based on global properties would fail to detect this damage, whereas the proposed method identified not only the existence but also the location of the damage.

ONGOING AND FUTURE WORK

While the localized damage detection method has been shown to be effective for the scenarios presented, it is important to continue to verify this method for increasingly complex and realistic structures. Although only one damage scenario is presented for the two-span girder simulation, ongoing research involves the investigation of a variety of damage combinations and loading cases. Also, an experimental prototype similar to the simulated girder will be constructed and tested at Lehigh University using three types of sensors: tethered piezoelectric accelerometers, wireless piezoelectric accelerometers, and strain gauges. Moreover, it is important to determine the smallest amount of damage to which this algorithm is sensitive.

ACKNOWLEDGMENTS

The research described in this paper is partially supported by the National Science Foundation through Grant No. CMMI-0926898 by Sensors and Sensing Systems program, and by a grant from the Commonwealth of Pennsylvania, Department of Community and Economic Development, through the Pennsylvania Infrastructure Technology Alliance (PITA).

REFERENCES

Alvandi, A., and Cremona, C. "Assessment of vibration-based damage." *Journal of Sound and Vibration* 292 (2006) 179–202.

Bernal, D., M.ASCE. "Load Vectors for Damage Localization." *Journal of Engineering Mechanics* (Jan 2002): 7-14.

Chen, J., and Gupta, A.K. (2000). *Parametric change point analysis*. Birkhäuser, Boston.

Doebling, Scott W., Farrar, Charles R., and Prime, Michael B. "A Summary Review of Vibration-Based Damage Identification Methods." *The Shock and Vibration Digest* 30 (Mar 1998): 91-105.

Koh, C.G., See, L.M., and Balendra, T. "Damage Detection of Buildings: Numerical and Experimental Studies." *J. Struct. Engrg.* 121(8), (Aug 1995): 1155-1160.

Labuz, E. L., Chang, M., Pakzad, S. "Local Damage Detection in Beam-Column Connections Using a Dense Sensor Network," *Proc. of 19th Annual Structures Congress*, Orlando, FL (May 2010).

Morassi, A., and Rovere, N. "Localizing a Notch in a Steel Frame from Frequency Measurements." *J. Engrg. Mech.* 123(5) (May 1997): 422-432.

Ratcliffe, C.P. "Damage Detection Using a Modified Laplacian Operator on Mode Shape Data." *Journal of Sound and Vibration* 204(3) (1997): 505-517.

Sohn, H., and Law, K.H. "A Bayesian Probabilistic Approach for Structure Damage Detection." *Earthquake Engineering and Structural Dynamics* 26 (1997): 1259-1281.

Trimm, Marvin. "An overview of nondestructive evaluation methods." *Journal of Failure Analysis and Prevention* 3(3) (2003): 17-31.

Yoon, M.K., Heider, D., Gillespie Jr., J.W., *et al.* "Local damage detection using the two-dimensional gapped smoothing method." *Journal of Sound and Vibration* 279 (2005): 119-139.